

# Modeling and Analysis of the Cutting Force Components in the Hard Milling of Hardened Cr12MoV Steel

**Trieu Quy Huy**

University of Economics and Technology for Industries, Vinh Tuy Ward, Hanoi, Vietnam  
tqhuy@uneti.edu.vn (corresponding author)

Received: 10 January 2026 | Revised: 25 February 2026 and 18 March 2026 | Accepted: 19 March 2026

Licensed under a CC-BY 4.0 license | Copyright (c) by the authors | DOI: <https://doi.org/10.48084/etasr.17456>

## ABSTRACT

**In the tough milling of hardened tool steels, cutting forces significantly affect process stability, tool wear, and spindle load. This study experimentally explores the orthogonal cutting force components ( $F_x$ ,  $F_y$ ,  $F_z$ ) during hard milling of hardened Cr12MoV steel (48-52 HRC) using TiAlN-coated carbide inserts. Central Composite Design (CCD) combined with Response Surface Methodology (RSM) was used to model the effects of cutting speed and feed rate. Second-order regression models were created and statistically validated with Analysis of Variance (ANOVA). The results show that cutting speed decreases forces mainly due to thermal softening, while feed rate raises forces mainly because of increased chip thickness. Among the components,  $F_y$  is the most sensitive to dynamic excitation. Based on these models, a stable cutting window is proposed for industrial use. The findings offer a dependable empirical basis for force prediction and the safe selection of parameters in finish hard milling of Cr12MoV die steel.**

**Keywords-hard milling; cutting force; Cr12MoV; CCD; RSM; TiAlN tool**

## I. INTRODUCTION

High-speed and hard milling of hardened tool steels is a key manufacturing strategy in the die and mold industry, as it can replace grinding while maintaining high productivity and dimensional accuracy [1-3]. However, machining materials with hardness above 45–50 HRC presents significant challenges, including high cutting forces, unstable chip formation, and accelerated tool wear, all of which can degrade surface integrity and process reliability [1, 4]. Among the various process variables, cutting force is one of the most crucial factors influencing machining performance, as it directly affects tool deflection, vibration behavior, spindle loading, and surface quality [5-7]. In milling operations, cutting forces are inherently dynamic due to intermittent tooth engagement, making accurate prediction and control of force components essential for ensuring process stability and avoiding chatter [7-9]. Consequently, numerous analytical and mechanistic models have been developed to predict milling forces and stability limits, emphasizing the role of force coefficients in dynamic machining systems [8–10]. In hard milling applications, tool material and coating play an important role in cutting performance. TiAlN-coated carbide tools are widely used due to their excellent thermal stability and wear resistance, which enhance cutting efficiency under high-temperature conditions [11-13]. Both tool wear mechanisms and cutting force evolution in hardened steels are strongly influenced by cutting parameters and coating properties [12, 13].

Cr12MoV steel is a typical cold-work die steel characterized by high hardness and wear resistance after heat treatment, making it difficult to machine. The hard milling of Cr12MoV often results in high cutting forces and force fluctuations, which may lead to instability and reduced machining quality [14]. Although the machining performance of hardened steels has been investigated, systematic modeling of orthogonal cutting force components ( $F_x$ ,  $F_y$ ,  $F_z$ ) for Cr12MoV under controlled experimental design conditions is limited. To address complex nonlinear relationships in machining processes, statistical modeling approaches such as Response Surface Methodology (RSM) have been widely employed. Central Composite Design (CCD) enables the efficient construction of second-order regression models with a limited number of experiments, rendering it suitable for machining studies where experimental costs are high [15-17]. CCD-RSM frameworks have been successfully deployed to model machining responses and optimize process parameters in advanced manufacturing applications [16, 17]. Optimization and modeling techniques based on experimental design and numerical approaches have been applied in modern manufacturing research, including welding, additive manufacturing, and CNC machining processes [18-24]. These studies demonstrate the effectiveness of CCD in capturing nonlinear process behavior and improving predictive capability.

Despite these advances, there are two important gaps. First, most existing studies focus on the resultant cutting force. In contrast, analysis of the individual orthogonal components ( $F_x$ ,

$F_y, F_z$ ) is limited, even though these components provide deeper insights into tool stability, vibration sensitivity, and spindle loading. Second, there is a lack of experimentally validated models, specifically developed for hardened Cr12MoV steel, using TiAlN-coated carbide tools within practical industrial parameter ranges. Therefore, this study aims to experimentally investigate the orthogonal cutting force components in hard milling of hardened Cr12MoV steel and to develop second-order regression models using CCD-RSM. The models are statistically validated using Analysis of Variance (ANOVA) and are further utilized to identify stable cutting conditions for industrial applications.

## II. METHODOLOGY

### A. Experimental Design

To establish statistically reliable predictive models with a limited number of experiments, a CCD within the RSM framework was employed. This design was selected because it efficiently captures linear, interaction, and quadratic effects of the input variables while reducing experimental cost. Two machining parameters were considered as independent variables: cutting speed  $V$  (m/min) and feed rate  $f$  (mm/min). These factors were selected based on a literature review, preliminary trials, and the tool manufacturer's recommendations, as they are known to significantly affect cutting force behavior in hard milling. Other machining conditions, including tool geometry, axial and radial depth of cut, cooling conditions, and milling strategy, were kept constant throughout the study to isolate the effects of  $V$  and  $f$ . The workpiece's hardness was measured at multiple points ( $n = 5$ ) using a Rockwell hardness tester before machining. The values ranged from 47.8 to 52.6 HRC, with an average of  $50.3 \pm 1.6$  HRC. Since all specimens came from the same batch, the hardness variation was minimal and had little impact on the measured cutting force components. A reduced face-centered CCD was adopted for the two-factor design. The experimental design consisted of 9 runs, including 4 factorial points, 4 axial points, and 1 center point, providing sufficient information to estimate quadratic effects and evaluate experimental error. The actual values of the variables were transformed into coded values according to:

$$x_i = \frac{X_i - X_0}{\Delta X_i}$$

where  $x_i$  is the coded value,  $X_i$  is the actual value of the factor,  $X_0$  is the value at the design center, and  $\Delta X_i$  is the step size. This coding procedure eliminates unit effects and facilitates comparison of regression coefficients.

The selected ranges of machining parameters were chosen to ensure stable cutting conditions while maintaining practical relevance for finish hard milling. According to the CCD matrix, the measured responses consisted of the three orthogonal cutting force components:  $F_x$ ,  $F_y$ , and  $F_z$ . The experimental design matrix, along with the corresponding measured force components, is presented in Table I. The results reveal significant variation in all three force components across the investigated parameter domain, indicating a strong sensitivity of the cutting process to changes in machining conditions.

TABLE I. EXPERIMENTAL DESIGN MATRIX AND MEASURED FORCE COMPONENTS

Run	V (m/min)	f (mm/min)	F <sub>x</sub> (N)	F <sub>y</sub> (N)	F <sub>z</sub> (N)
1	60	170	424.17	386.37	380.48
2	80	200	200.15	180.81	150.32
3	60	230	495.35	473.25	418.34
4	80	120	250.31	248.50	252.81
5	50	200	582.05	567.11	491.52
6	100	230	186.25	224.13	200.28
7	100	170	155.34	188.23	171.47
8	110	200	163.72	158.79	160.26
9	80	280	336.52	300.48	264.61

### B. Experimental Setup

All experiments were performed on a vertical CNC machining center under stable operating conditions. The workpiece material was hardened Cr12MoV steel with a hardness of approximately 50 HRC. Machining was carried out using a TiAlN-coated carbide end mill with constant tool geometry throughout the study. Milling operations were conducted under down-milling (climb milling) conditions, which are commonly preferred in finish hard milling due to their superior cutting stability and improved surface quality. To isolate the effects of cutting speed and feed rate, the axial and radial depths of cut were kept constant during all experiments.

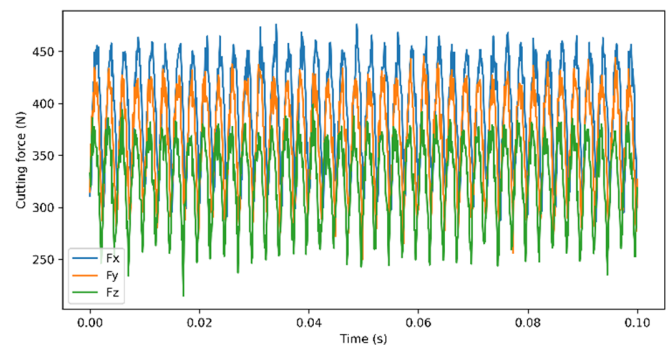


Fig. 1. Typical cutting force signal in the time domain.

Figure 1 shows the dynamic nature of the milling process and the vibration-supported cutting system, presenting typical force signals in the time domain. Cutting forces were measured using a three-component piezoelectric dynamometer (Kistler 9257B) mounted rigidly between the workpiece and the machine table. The force signals in the three orthogonal directions ( $F_x$ ,  $F_y$ ,  $F_z$ ) were acquired using a high-frequency data acquisition system with a sampling frequency of 5-10 kHz. To ensure measurement reliability, signals were recorded after the cutting process reached steady-state conditions (after 2-3 tool engagements). A low-pass filter was applied to remove high-frequency noise, and the final force values were obtained by time-averaging the steady-state signals. Flood cooling using a water-soluble emulsion (5%) was applied during all experiments to maintain thermal stability and simulate practical industrial conditions. In addition to force measurements, surface roughness ( $R_a$ ) and cutting temperature ( $T$ ) were monitored during the experiments to ensure process consistency and thermal stability. However, these variables

were not included in the RSM modeling, as the present study focuses on the dominant effects of cutting speed and feed rate on cutting force components.

### C. Modeling Approach

To describe the relationship between machining parameters and cutting force components, a second-order regression model based on RSM was employed. This approach enables the characterization of linear, interaction, and quadratic effects of the input variables within the investigated domain. For each response ( $F_x$ ,  $F_y$ ,  $F_z$ ), the general form of the quadratic model is expressed as:

$$F_i = \beta_0 + \beta_1 V + \beta_2 f + \beta_{12} Vf + \beta_{11} V^2 + \beta_{22} f^2$$

where  $Y$  represents the cutting force component,  $V$  is the cutting speed,  $f$  is the feed rate, and  $\beta_i$  are the regression coefficients determined using the least-squares method.

The adequacy and statistical significance of the developed models were evaluated using ANOVA at a 95% confidence level. A model was considered statistically significant when the p-value was less than 0.05, while a non-significant lack-of-fit ( $p > 0.05$ ) indicated good agreement between the model and experimental data. Model reliability was further verified using standard statistical indicators, including the coefficient of determination ( $R^2$ ) and adjusted coefficient of determination ( $R^2_a$ ), which quantify the proportion of variance explained by the model. The developed models are empirical and valid within the investigated parameter range. They are intended for predictive and optimization purposes rather than for establishing a full mechanistic description of the cutting process.

## III. RESULTS AND DISCUSSION

### A. Model Adequacy

The adequacy of the developed second-order regression models for the cutting force components ( $F_x$ ,  $F_y$ , and  $F_z$ ) was assessed using ANOVA and standard statistical indicators. The results showed that all models have high predictive accuracy, with coefficients of determination around  $R^2 = 0.99$  for  $F_x$ ,  $R^2 = 0.96$  for  $F_y$ , and  $R^2 = 0.96$  for  $F_z$ . These values confirm that the models effectively capture the relationship between machining parameters and the corresponding force components within the studied domain. The ANOVA results indicated that the overall models are statistically significant at the 95% confidence level ( $p < 0.05$ ). Specifically,  $V$  and its quadratic term ( $V^2$ ) are the main factors influencing the cutting force components.

In contrast, the  $f$  is not statistically significant within the examined parameter range ( $p > 0.05$ ). However, it still plays an important physical role in determining the magnitude of the cutting force. This distinction emphasizes the difference between statistical contribution and physical significance under the chosen experimental conditions. Additionally, the lack-of-fit tests are not statistically significant ( $p > 0.05$ ), indicating that the models adequately represent the experimental data without systematic errors. The agreement between ANOVA results and the high  $R^2$  values confirms that the proposed CCD-RSM models are reliable for predicting orthogonal cutting force components in hard milling of Cr12MoV steel.

### B. ANOVA Analysis

TABLE II. ANOVA RESULTS FOR QUADRATIC MODELS OF  $F_x$ ,  $F_y$ , AND  $F_z$

Source	DF	$F_{xF}$	$F_{xP}$	$F_{yF}$	$F_{yP}$	$F_{zF}$	$F_{zP}$
V	1	28.87	0.0126	6.68	0.0814	8.41	0.0625
f	1	1.69	0.2848	0.19	0.6904	1.12	0.3671
Vxf	1	0.80	0.4380	0.32	0.6118	0.01	0.9204
$V^2$	1	36.75	0.0090	9.51	0.0539	10.02	0.0507
$f^2$	1	9.10	0.0569	1.66	0.2878	2.64	0.2025
Error	3	—	—	—	—	—	—

Note: Terms with  $p < 0.05$  are considered statistically significant at the 95% confidence level.  
 $F_xF = F_x$ : F-value;  $F_{xP} = F_x$ : p-value;  $F_{yF} = F_y$ : F-value;  $F_{yP} = F_y$ : p-value;  $F_{zF} = F_z$ : F-value;  $F_{zP} = F_z$ : p-value;

ANOVA was performed to quantify the effects of machining parameters and their interactions on the cutting force components  $F_x$ ,  $F_y$ , and  $F_z$ , as summarized in Table II. The results indicate that cutting speed  $V$  has a statistically significant effect on the cutting forces, particularly on  $F_x$  ( $p < 0.05$ ). The quadratic term  $V^2$  is also significant, confirming the nonlinear relationship between cutting speed and the force components. In contrast, the feed rate  $f$  is not statistically significant within the examined range ( $p > 0.05$ ). However, from a physical standpoint, it still plays an important role by increasing the uncut chip thickness and, consequently, the magnitude of the cutting forces. This highlights the distinction between statistical significance and physical influence within the investigated domain. Furthermore, the linear term of  $f$ , its interaction with cutting speed ( $V \times f$ ), and its quadratic term ( $f^2$ ) are all statistically insignificant ( $p > 0.05$ ), indicating that cutting speed is the dominant factor governing variations in the cutting force components within the studied range. Despite this, increasing the feed rate leads to higher cutting loads due to the enlargement of the shear area and intensified plastic deformation. The observed discrepancy between statistical and physical significance can be attributed to the relatively narrow parameter range and the limited number of experimental runs in the CCD design. Overall, the ANOVA results confirm that the developed models are primarily driven by cutting speed and its nonlinear effects, while feed rate acts as a secondary factor with strong practical relevance but limited statistical contribution under the selected conditions.

### C. Effect of Cutting Parameters

The influence of cutting parameters on the orthogonal  $F_x$ ,  $F_y$ , and  $F_z$  was analyzed using the developed RSM models and experimental observations.  $V$  shows a negative correlation with all force components, indicating that cutting forces decrease as cutting speed increases. This behavior is mainly attributed to the thermal softening effect in the cutting zone. At higher cutting speeds, the increased temperature reduces the material flow stress, facilitating chip formation and lowering cutting forces.

A significant reduction in force is observed as the cutting speed increases from low to high. This effect is especially noticeable for  $F_y$ , which is more sensitive to shear deformation and friction conditions. At very high cutting speeds, the rate of force reduction slows due to increased friction at the tool-chip interface.  $f$  has a strong positive effect on the size of the cutting force. Raising the feed rate results in a thicker uncut chip,

leading to higher cutting forces due to more plastic deformation and friction. Although the feed rate is not statistically significant in ANOVA, its practical impact is evident. Higher feed rates also cause increased force fluctuations, leading to vibrations and less stable machining. The combined analysis shows that cutting speed mainly drives the reduction in force, while feed rate influences the magnitude of the latter.

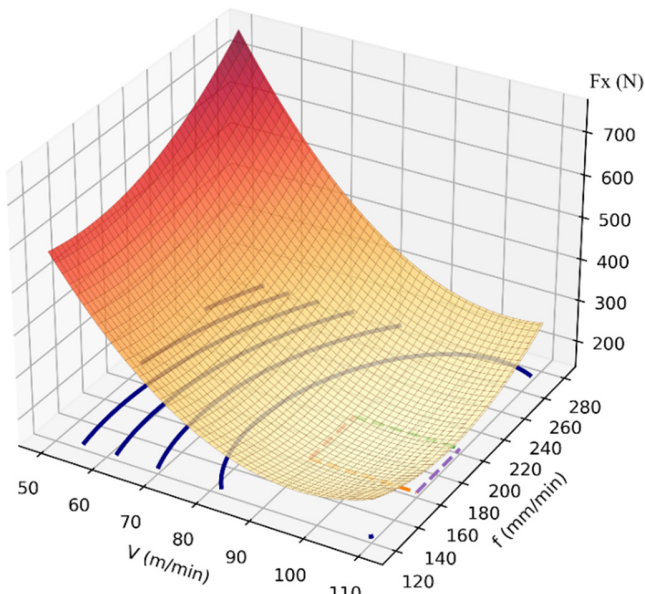


Fig. 2. Graph of the force component  $F_x$  relative to  $V$  and  $f$ .

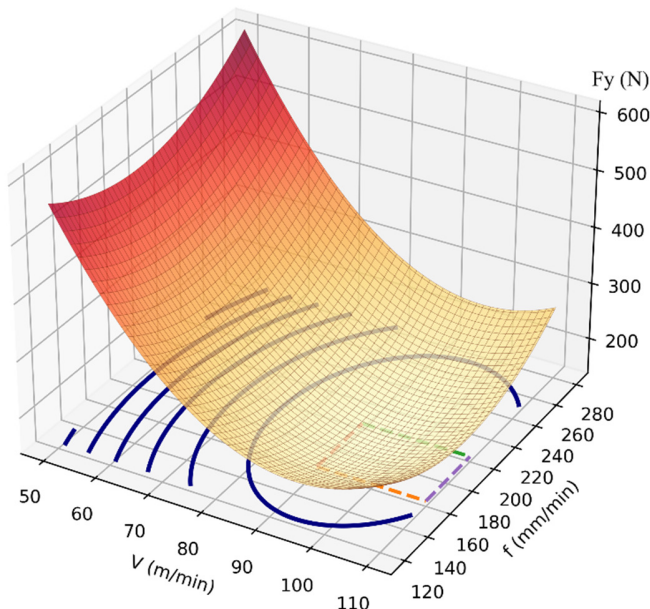


Fig. 3. Graph of the force component  $F_y$  relative to  $V$  and  $f$ .

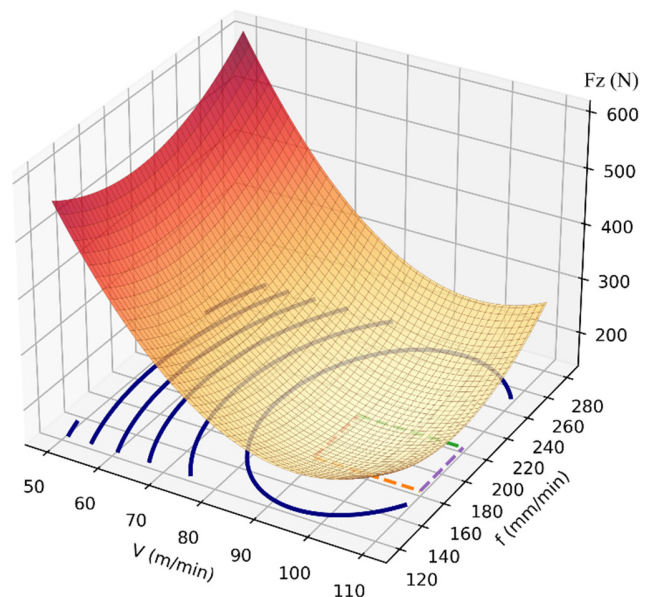


Fig. 4. Graph of the force component  $F_z$  relative to  $V$  and  $f$ .

In Figures 2-4, a relatively stable region is observed at high cutting speeds and moderate feed rates, where all force components remain moderate.

#### D. Interpretation of Force Components

Breaking down the resulting cutting force into three perpendicular components ( $F_x$ ,  $F_y$ , and  $F_z$ ) provides a clearer understanding of the mechanical behavior in hard milling, as each component represents a distinct aspect of machining performance. The feed-direction force ( $F_x$ ) is mainly associated with tool trajectory stability. Variations in  $F_x$  directly influence the tool's instantaneous displacement in the feed direction, thereby affecting dimensional accuracy and surface integrity. Due to its relatively stable behavior and high model adequacy,  $F_x$  can be considered a reliable indicator of process consistency. The transverse force ( $F_y$ ) plays a dominant role in the dynamic stability of the machining system. This component is responsible for the lateral excitation of the tool-workpiece system and is closely linked to vibration and chatter phenomena. An increase in  $F_y$ , particularly at high feed rates, indicates a higher risk of instability, rendering it a crucial parameter for evaluating machining stability. The axial force ( $F_z$ ) represents the load transmitted along the spindle axis and is directly related to spindle bearing loading and machine durability. Although its magnitude is generally lower than that of  $F_x$  and  $F_y$ , its continuous action along the spindle direction can significantly affect long-term machine performance and operational safety. From an engineering perspective, the simultaneous consideration of these three force components enables a more comprehensive evaluation of machining conditions. Specifically,  $F_x$  governs geometric accuracy,  $F_y$  determines vibration risk, and  $F_z$  reflects spindle load. Therefore, optimal cutting conditions should be selected by balancing these components rather than minimizing a single resultant force.

### E. Force Generation in Hard Milling

Beyond statistical modeling, the observed variation in cutting force components can also be interpreted from a mechanistic perspective, based on chip formation and energy dissipation in the cutting zone. In hard milling of hardened Cr12MoV steel, the cutting process involves a combined mechanism of shearing and ploughing, particularly at low effective cutting speeds. The resultant cutting force can be expressed as a combination of shear force and ploughing force:

$$F = F_s + F_p$$

where  $F_s$  is associated with shear deformation along the primary shear zone, and  $F_p$  represents ploughing and friction effects along the tool flank and rake faces.

At low cutting speeds, the temperature in the cutting zone is insufficient to soften the material, leading to a higher flow stress. As a result, the ploughing component becomes dominant, especially near the tool tip where the effective cutting radius approaches zero. This explains the elevated force levels observed at low cutting speeds. As cutting speed increases, thermal softening reduces the material's shear strength, thereby decreasing  $F_s$ . Simultaneously, improved chip formation reduces the ploughing contribution, leading to an overall reduction in cutting force components.

The feed rate, on the other hand, directly controls the uncut chip thickness  $h$ , approximated as  $h \propto f_z$ . An increase in feed rate results in a larger shear area, and thus higher cutting forces. However, within the investigated parameter range, the variation in feed rate is insufficient to produce a statistically significant effect in the ANOVA, despite its strong physical influence. From a dynamic perspective, the transverse force component  $F_y$  is the primary excitation source in the tool's radial direction, contributing to regenerative vibration and chatter instability. Therefore, controlling  $F_y$  is significant for ensuring stable machining conditions. This mechanistic interpretation complements the CCD-RSM models by providing a physical explanation for the observed statistical trends, thereby enhancing the robustness and generalizability of the proposed predictive framework.

### F. Optimal Cutting Conditions

Based on the developed RSM models and the analysis of cutting force components, an optimal cutting region for finish hard milling of hardened Cr12MoV steel was identified within the investigated parameter domain. The results indicate that a combination of relatively high cutting speed and moderate feed rate provides the most favorable machining conditions. Specifically, a cutting speed range of  $V = 90$  m/min–110 m/min and a feed rate range of  $f = 160$  m/min–200 m/min result in moderate values of  $F_x$ ,  $F_y$ , and  $F_z$ , thereby reducing the risk of vibration and excessive spindle loading while maintaining machining efficiency. From a mechanistic standpoint, higher cutting speeds promote thermal softening of the workpiece material, leading to reduced cutting forces. In contrast, moderate feed rates limit the increase in uncut chip thickness, preventing excessive mechanical loading. This balance is essential for achieving stable cutting conditions in hard milling operations. Conversely, combinations of low

cutting speed and high feed rate should be avoided, as they produce elevated cutting forces and increase the likelihood of vibration, accelerated tool wear, and process instability. Overall, the identified parameter window provides a practical guideline for selecting cutting conditions that ensure stable operation, reduced cutting forces, and improved machining reliability in industrial applications.

## IV. CONCLUSIONS

This study developed and validated second-order Central Composite Design-Response Surface Methodology (CCD-RSM) models to predict the orthogonal cutting force components ( $F_x$ ,  $F_y$ , and  $F_z$ ) in the hard milling of hardened Cr12MoV steel using TiAlN-coated carbide tools. The models exhibited high predictive accuracy ( $R^2$  up to 0.99) and strong statistical reliability, as confirmed by Analysis of Variance (ANOVA) and lack-of-fit tests. The results demonstrate that cutting speed reduces cutting forces primarily due to thermal softening, whereas feed rate governs force magnitude through its influence on uncut chip thickness. A key finding is the distinction between statistical and physical significance: cutting speed dominates the model behavior, while feed rate remains the primary factor controlling the practical magnitude of the cutting forces. Analysis of the individual force components provides further engineering insights into machining performance, with  $F_x$  associated with trajectory stability,  $F_y$  linked to vibration and chatter risk, and  $F_z$  related to spindle loading. An optimal cutting region ( $V = 90$  m/min–110 m/min and  $f = 160$  m/min–200 m/min) was identified to ensure stable and reliable machining conditions. Overall, these findings provide a practical basis for process parameter selection and contribute to improved stability, extended tool life, and enhanced machining efficiency in industrial hard milling applications.

## DECLARATION OF COMPETING INTERESTS

The author states that there are no known competing financial interests or personal relationships that could have influenced the work reported in this paper.

## ACKNOWLEDGMENT

The author would like to acknowledge the support of the University of Economics and Technology for Industries (UNETI) in providing experimental facilities and a research environment.

## DATA AVAILABILITY

The datasets generated and/or analyzed during this study are available from the corresponding author upon reasonable request.

## REFERENCES

- [1] H. K. Tönshoff, C. Arendt, and R. B. Amor, "Cutting of Hardened Steel," *CIRP Annals*, vol. 49, no. 2, pp. 547–566, Jan. 2000, [https://doi.org/10.1016/S0007-8506\(07\)63455-6](https://doi.org/10.1016/S0007-8506(07)63455-6).
- [2] W. Grzesik, "Machining of Hard Materials," in *Machining: Fundamentals and Recent Advances*, J. P. Davim, Ed. London: Springer, 2008, pp. 97–126.

- [3] H. Schulz and T. Moriwaki, "High-speed Machining," *CIRP Annals*, vol. 41, no. 2, pp. 637–643, Jan. 1992, [https://doi.org/10.1016/S0007-8506\(07\)63250-8](https://doi.org/10.1016/S0007-8506(07)63250-8).
- [4] W. A. Kline, R. E. DeVor, and J. R. Lindberg, "The prediction of cutting forces in end milling with application to cornering cuts," *International Journal of Machine Tool Design and Research*, vol. 22, no. 1, pp. 7–22, Jan. 1982, [https://doi.org/10.1016/0020-7357\(82\)90016-6](https://doi.org/10.1016/0020-7357(82)90016-6).
- [5] N. D. Sims, B. Mann, and S. Huyanan, "Analytical prediction of chatter stability for variable pitch and variable helix milling tools," *Journal of Sound and Vibration*, vol. 317, no. 3, pp. 664–686, Nov. 2008, <https://doi.org/10.1016/j.jsv.2008.03.045>.
- [6] P. Lee and Y. Altıntaş, "Prediction of ball-end milling forces from orthogonal cutting data," *International Journal of Machine Tools and Manufacture*, vol. 36, no. 9, pp. 1059–1072, Sept. 1996, [https://doi.org/10.1016/0890-6955\(95\)00081-X](https://doi.org/10.1016/0890-6955(95)00081-X).
- [7] Y. Altıntaş and E. Budak, "Analytical Prediction of Stability Lobes in Milling," *CIRP Annals*, vol. 44, no. 1, pp. 357–362, Jan. 1995, [https://doi.org/10.1016/S0007-8506\(07\)62342-7](https://doi.org/10.1016/S0007-8506(07)62342-7).
- [8] E. Budak and Y. Altıntaş, "Analytical Prediction of Chatter Stability in Milling—Part I: General Formulation," *Journal of Dynamic Systems, Measurement, and Control*, vol. 120, no. 1, pp. 22–30, Mar. 1998, <https://doi.org/10.1115/1.2801317>.
- [9] E. Budak and Y. Altıntaş, "Analytical Prediction of Chatter Stability in Milling—Part II: Application of the General Formulation to Common Milling Systems," *Journal of Dynamic Systems, Measurement, and Control*, vol. 120, no. 1, pp. 31–36, Mar. 1998, <https://doi.org/10.1115/1.2801318>.
- [10] V. F. C. Sousa, F. J. G. D. Silva, G. F. Pinto, A. Baptista, and R. Alexandre, "Characteristics and Wear Mechanisms of TiAlN-Based Coatings for Machining Applications: A Comprehensive Review," *Metals*, vol. 11, no. 2, Feb. 2021, <https://doi.org/10.3390/met11020260>.
- [11] C. Y. Wang, Y. X. Xie, Z. Qin, H. S. Lin, Y. H. Yuan, and Q. M. Wang, "Wear and breakage of TiAlN- and TiSiN-coated carbide tools during high-speed milling of hardened steel," *Wear*, vol. 336–337, pp. 29–42, Aug. 2015, <https://doi.org/10.1016/j.wear.2015.04.018>.
- [12] S. Wu, G. Liu, W. Zhang, W. Chen, and C. Wang, "High-speed milling of hardened steel under minimal quantity lubrication with liquid nitrogen," *Journal of Manufacturing Processes*, vol. 95, pp. 351–368, June 2023, <https://doi.org/10.1016/j.jmapro.2023.04.013>.
- [13] F. Sun, G. Li, Q. Zhang, and M. Liu, "Research on High-speed Cutting of Cr12MoV Hardened Steel - A Review," *Recent Patents on Engineering*, vol. 16, no. 1, pp. 47–58, Jan. 2022, <https://doi.org/10.2174/1872212115999201201111251>.
- [14] J. Ma, X. L. Liu, C. X. Yue, F. Liu, and G. Y. Wang, "Characteristic Study of Milling Force in Cut-In Process of Hard Milling Die Steel," *Key Engineering Materials*, vol. 589–590, pp. 147–151, 2014, <https://doi.org/10.4028/www.scientific.net/KEM.589-590.147>.
- [15] G. E. P. Box and K. B. Wilson, "On the Experimental Attainment of Optimum Conditions," in *Breakthroughs in Statistics: Methodology and Distribution*, S. Kotz and N. L. Johnson, Eds. New York, NY: Springer, 1992, pp. 270–310.
- [16] R. D. Patel and S. N. Bhavsar, "Experimental investigation during end milling of AISI D2 tool steel using AlCrN coated tool," *Materials Today: Proceedings*, vol. 22, pp. 2647–2656, Jan. 2020, <https://doi.org/10.1016/j.matpr.2020.03.396>.
- [17] C. Sukkam and S. Chajit, "Investigation of Influencing Factors on Surface Quality during Low-Speed Cutting of Steels with a Hardness exceeding 50 HRC for forging Dies," *Engineering, Technology & Applied Science Research*, vol. 14, no. 3, pp. 14056–14061, June 2024, <https://doi.org/10.48084/etasr.7079>.
- [18] D. A. Efa, "Laser Beam Welding Parametric Optimization for AZ31B and 6061-T6 Alloys: Residual Stress and Temperature Analysis Using a CCD, GA and ANN," *Optics & Laser Technology*, vol. 175, Aug. 2024, Art. no. 110837, <https://doi.org/10.1016/j.optlastec.2024.110837>.
- [19] D. A. Efa, "Enhancing the efficiency of laser beam welding: multi-objective parametric optimization of dissimilar materials using finite element analysis," *The International Journal of Advanced Manufacturing Technology*, vol. 133, no. 9, pp. 4525–4541, Aug. 2024, <https://doi.org/10.1007/s00170-024-13985-y>.
- [20] D. A. Efa and D. A. Ifa, "Optimization of design parameters and 3D-printing orientation to enhance the efficiency of topology-optimized components in additive manufacturing," *Results in Materials*, vol. 26, June 2025, Art. no. 100702, <https://doi.org/10.1016/j.rinma.2025.100702>.
- [21] L. D. Gemechu, D. A. Efa, and R. Abebe, "Optimizing CNC turning of AISI D3 tool steel using Al<sub>2</sub>O<sub>3</sub>/graphene nanofluid and machine learning algorithms," *Heliyon*, vol. 10, no. 24, Dec. 2024, <https://doi.org/10.1016/j.heliyon.2024.e40969>.
- [22] D. A. Efa, N. D. Dejene, D. A. Ifa, S. K. Nemomsa, and T. B. Gemechu, "Improving computer numerical control (CNC) turning performance of AISI D2 steel with nanofluid composites and advanced machine learning techniques," *The International Journal of Advanced Manufacturing Technology*, vol. 138, no. 2, pp. 511–539, May 2025, <https://doi.org/10.1007/s00170-025-15536-5>.
- [23] D. A. Ifa, D. A. Efa, N. D. Dejene, and S. K. Nemomsa, "Physics-informed modeling and process optimization of friction stir welding of AA7075-T6 with a zinc interlayer," *Next Materials*, vol. 9, Oct. 2025, Art. no. 100999, <https://doi.org/10.1016/j.nxmate.2025.100999>.
- [24] D. A. Efa, D. A. Ifa, N. D. Dejene, H. Z. Belachew, and D. F. Tegegn, "Sol-gel and co-precipitation synthesized hybrid nanofluids for enhanced CNC turning of AISI 4340 steel: an experimental and machine learning approach," *Scientific Reports*, vol. 15, no. 1, Nov. 2025, Art. no. 41207, <https://doi.org/10.1038/s41598-025-25102-4>.